Conf-950793--5

BNL-61928

Quantum Phase Space Theory for the Calculation of v·j Vector Correlations

Gregory E. Hall
Department of Chemistry, Brookhaven National Laboratory, Upton, NY 11973-5000

The quantum state-counting phase space theory commonly used to describe "barrierless" dissociation is recast in a helicity basis to calculate photofragment **v·j** correlations. Counting pairs of fragment states with specific angular momentum projection numbers on the relative velocity provides a simple connection between angular momentum conservation and the **v·j** correlation, which is not so evident in the conventional basis for phase space state counts. The upper bound on the orbital angular momentum, l, imposed by the centrifugal barrier cannot be included simply in the helicity basis, where l is not a good quantum number. Two approaches for a quantum calculation of the **v·j** correlation are described to address this point. An application to the photodissociation of NCCN is consistent with recent classical phase space calculations of Cline and Klippenstein. The observed vector correlation exceeds the phase space theory prediction. We take this as evidence of incomplete mixing of the K states of the linear parent molecule at the transition state, corresponding to an evolution of the body-fixed projection number K into the total helicity of the fragment pair state. The average over a thermal distribution of parent angular momentum in the special case of a linear molecule does not significantly reduce the **v·j** correlation below that computed for total $J = 0$.

keywords: phase space theory, helicity, vector correlations, photodissociation dynamics

I. Introduction

Phase space theory[1] offers a simple and intuitive reference point for viewing possible dynamic effects in unimolecular and bimolecular reactions. For reactions with no barriers, the transition state resembles separated product states, and a detailed transition state rate calculation can often be replaced by an appropriate state count of the products, consistent with energy and angular momentum conservation. Phase space theory has been compared with varying degrees of success to measured rotational and vibrational state distributions, translational energy distributions, threshold photofragment excitation spectra, and absolute reaction rates.[2, 3] The connection between phase space theory and vector correlations is less well known. Cline and Klippenstein[4] have recently used Monte Carlo methods to generate a representative classical phase space ensemble from which vector correlations have been inspected. They present useful generalizations about the statistical expectations for photofragment **v·j** correlations, based on the relative moments of inertia of two reaction products and on the total angular momentum.

In this work, the structure of quantum phase space theory is considered, using a traditional state-counting technique, but making explicit the statistical expectations for the **v·j** correlation. In the bipolar moment language applied by Dixon[5] to the Doppler spectroscopy of photofragments, the leading term in the **v·j** correlation is $\beta_0^0(22)$, which is the ensemble average of $P_2(\hat{\mathbf{v}}\cdot\hat{\mathbf{j}})$, where $P_2(x) = \frac{1}{2}(3x^2 - 1)$ and $\hat{\mathbf{v}}$ is the unit vector along the recoil velocity of a fragment with a rotational angular momentum in the direction $\hat{\mathbf{j}}$. Calculation of $\langle P_2(\hat{\mathbf{v}}\hat{\mathbf{j}})\rangle$ lends itself to working in a basis for which the projection of **j** on the relative velocity is a good quantum number. A helicity basis set, first described by Jacob and Wick[6] in the context of nuclear scattering theory for particles with intrinsic spin, has this property, and lends an intuitive simplicity to state counting when Legendre moments of the helicity are the desired observables.

II. Theory

The statistical phase space theory is applied to the breakup of a molecular complex with a specific energy E, and total angular momentum J. The probability of producing fragment I in electronic and vibrational state v_i and rotational state j_i is given by the number of such states, $N(v_i, j_i; E, J)$ normalized by the total number of accessible states $N(E,J)$:

DISTRIBUTION OF THIS DOCUMENT IS UNLIMITED MASTER

$$P_{v_i,j_i}(E,J) = \frac{N(v_i j_i;E,J)}{N(E,J)}. \tag{1}$$

Klippenstein[4] has provided a compact notation for the evaluation of the state counts for two nonlinear fragments:

$$N(E,J) = \sum_{v_1,j_1,k_1,v_2,j_2,k_2,l,j,m_J} \Theta[\, E - E_1(v_1,j_1,k_1) - E_2(v_2,j_2,k_2) - E_{12}^{\dagger}(l)] \times \Delta(J,j,l)\ \Delta(j,j_1,j_2) \tag{2}$$

where j_i and k_i are the angular momenta and their body-fixed projections for fragment I, l is the orbital angular momentum, j is the net angular momentum of $j_1 + j_2$ and m_J is a space-fixed projection of total angular momentum, J. The Heaviside function, Θ, ensures counting only states that conserve energy, including the l-dependent energy at the centrifugal barrier, $E_{12}^{\dagger}$. Angular momentum conservation is represented by a pair of triangle inequalities restricting the values of j and l for given j_1, j_2, and J. The energy at the top of the centrifugal barrier is written as

$$E_{12}^{\dagger}(l) = 2\left[\frac{l(l+1)\,\hbar^2}{6\mu\, C^{1/3}}\right]^{3/2} \tag{3}$$

where C is the coefficient of the spherically averaged, r^{-6} dependent, attractive interaction potential and μ is the reduced mass of the two fragments. This is appropriate at low kinetic energies, when the centrifugal barrier is at large enough fragment separation to ignore the contributions of chemical bonding and repulsion to the total interaction potential.

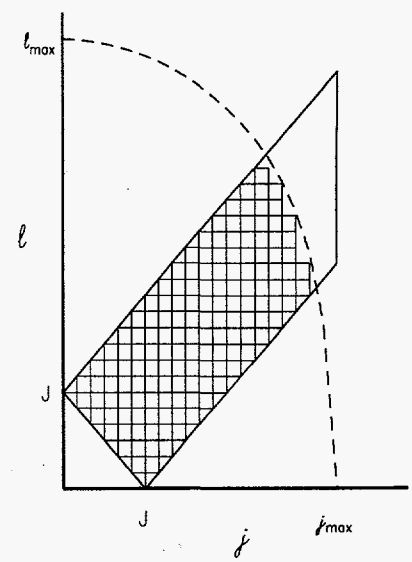

Figure 1 Conventional state count for A+BC at fixed total J comes from the number of interior $j\ l$ lattice points.

In the original formulation[1] for breakup of a triatomic complex, ABC→ A + BC, the only angular momenta involved are l for the orbital angular momentum, j for the diatomic rotation, and J for the total angular momentum. The state counts in this case are graphically depicted as the number of lattice points on the $j\ l$ plane. Figure 1 shows a typical $j\ l$ plane for fixed J. Three diagonal linear boundaries arise from angular momentum conservation, while the vertical line at j_{max} represents the total energy going into the rotation of BC. The dashed, curved boundary arises from energy conservation including the centrifugal barrier's upper bound on l.

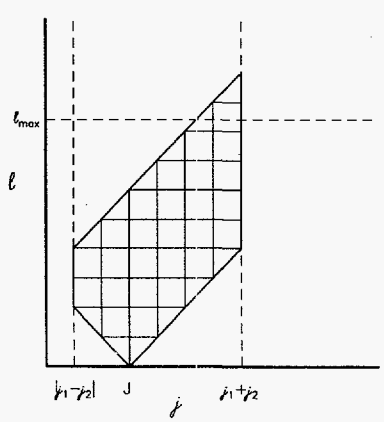

Figure 2. State count for a pair of diatomic fragments for fixed total J, j_1 and j_2.

The generalization to fragmentation of a four-atom complex into a pair of diatomic fragments has been treated by Dagdigian, *et al.*[7] and by Wittig, *et al.*[8]. The state counts are only slightly more complex, as indicated in Eq. (2). Now the counting can be graphically represented in Fig. 2 as lattice points on a $j\ l$ plane, where j is the resultant of $j_1 + j_2$, and the plot is for fixed values of J, j_1 and j_2. The upper and lower bounds on j are indicated as vertical dashed lines. Since the kinetic energy is the same for all the states counted in this figure, the upper bound on l is a

DISCLAIMER

This report was prepared as an account of work sponsored by an agency of the United States Government. Neither the United States Government nor any agency thereof, nor any of their employees, makes any warranty, express or implied, or assumes any legal liability or responsibility for the accuracy, completeness, or usefulness of any information, apparatus, product, or process disclosed, or represents that its use would not infringe privately owned rights. Reference herein to any specific commercial product, process, or service by trade name, trademark, manufacturer, or otherwise does not necessarily constitute or imply its endorsement, recommendation, or favoring by the United States Government or any agency thereof. The views and opinions of authors expressed herein do not necessarily state or reflect those of the United States Government or any agency thereof.

DISCLAIMER

Portions of this document may be illegible in electronic image products. Images are produced from the best available original document.

horizontal line, independent of j. The upper bound on l derived from the centrifugal barrier may or may not be more restrictive than the angular momentum restrictions alone.

A calculation of the vector correlation of fragment velocity and rotational angular momentum is awkward in this basis, implicit in Eq. 2, conventionally used in a phase space counting. Indeed, Cline and Klippenstein have resorted to a Monte Carlo calculation of classical phase space to address the identical question.[3] A helicity basis, as described by Jacob and Wick[6] lends itself to a direct quantum evaluation of the $\mathbf{v}\cdot\mathbf{j}$ correlation, since the projections of fragment angular momenta on the recoil axis are good quantum numbers in this basis. The l and j quantum numbers are abandoned in favor of helicity quantum numbers, λ_i, denoting the projections of angular momentum on the center-of-mass relative velocity. Along this unique axis, the orbital angular momentum necessarily has zero projection. A complete set of quantum numbers specifying the same breakup to two fragment states includes total J and its space-fixed projection number M, the magnitudes of two fragment angular momenta, j_1 and j_2, and the two fragment helicities, λ_1 and λ_2. The total helicity, $\Lambda = \lambda_1 - \lambda_2$ is independent of the orbital angular momentum. If we neglect, for the moment, the upper bound on l due to the centrifugal barrier, we can define $N'(E,J) \geq N(E,J)$ as upper bound on the true phase space state count obtained by dropping the centrifugal energy term, $E_{l2}^{\dagger}$.

$$N'(E,J) = \sum_{v_1,j_1,k_1,v_2,j_2,k_2,l,j,m_J} \Theta[\, E - E_1(v_1,j_1,k_1) - E_2(v_2,j_2,k_2)] \times \Delta(J,j,l)\ \Delta(j,j_1,j_2) \tag{4}$$

This same sum can be evaluated in the helicity basis:

$$N'(E,J) = \sum_{v_1,j_1,k_1,\lambda_1,v_2,j_2,k_2,\lambda_2,m_J} \Theta[\, E - E_1(v_1,j_1,k_1) - E_2(v_2,j_2,k_2)] \times \Theta(J - |\lambda_1 - \lambda_2|). \tag{5}$$

The triangle inequalities involving l and j have been replaced by upper and lower bounds on the total helicity Λ. It is to be understood that the summations over projection numbers λ_i and k_i are bounded by $\pm j_i$. It can be verified that the corresponding state count is identical in this helicity basis and in the conventional basis. A few simple examples are shown in the next section. From here on, I will drop reference to body-fixed projection numbers k_i, and specialize the discussion to diatomic fragments.

The conventional $l\,j$ states can be expanded in the helicity basis for each fixed j_1 and j_2. The elements of the transformation matrix are given by Jacob and Wick[6]:

$$\langle JM;lj|JM;\lambda_1\lambda_2\rangle = \left(\frac{2l+1}{2J+1}\right)^{1/2} C(j_1j_2j;\lambda_1,-\lambda_2)\ C(ljJ;0,\Lambda). \tag{6}$$

The first Clebsch-Gordon coefficient treats the coupling of j_1 and j_2 in specific helicity states to give a net angular momentum j and total helicity $\lambda_1 - \lambda_2$; the second reflects the fact that only the $m_l = 0$ component of the orbital angular momentum need be considered when coupling j and l in the helicity frame. The transformation is unitary, and gives us immediately, if inefficiently, a method to calculate the quantum phase space prediction for the $\mathbf{v}\cdot\mathbf{j}$ correlation for a fragment in state j_1. The prescription follows: count the states in the $l\,j$ basis according to Eq. 2, and transform each $l\,j$ state into its mixed helicity components according to Eq. 6. Accumulate the probability distribution of λ_1 in a histogram, $p(\lambda_1)$, for each $l\,j$ state included in the conventional phase space state count. When all $l\,j$ states have been included in the sum, the desired $\mathbf{v}\cdot\mathbf{j}$ correlation is simply the second Legendre moment of the normalized $p(\lambda_1)$ distribution:

$$\langle P_2(\hat{\mathbf{v}}\cdot\hat{\mathbf{j}}_1)\rangle = \sum_{\lambda_1=-j_1}^{j_1} p(\lambda_1)\cdot P_2\left(\frac{\lambda_1}{\sqrt{j_1(j_1+1)}}\right). \tag{7}$$

While straightforward, this procedure includes calculating many Clebsch-Gordon coefficients for each $l\,j$ state in the count of $N(E,J)$. The calculation can be made much more compact, avoiding most of the transformations, by approaching the problem directly in the helicity basis for a first approximation. We can instead compute $p'(\lambda_1)$ directly from the count of $\lambda_1\ \lambda_2$ states for a given selected state of fragment 1: j_1 and v_1, normalized by the appropriate total count for that state, $N'(v_1, j_1; E, J)$.

$$p'(\lambda_1;E,J,\mathrm{v}_1,j_1) = \frac{(2J+1)}{N'(\mathrm{v}_1,j_1;\ E,J)} \sum_{\mathrm{v}_2,j_2,\lambda_2} \Theta[\ E-E_1(\mathrm{v}_1,j_1)-E_2(\mathrm{v}_2,j_2)] \times \Theta(J-|\lambda_1-\lambda_2)] \tag{8}$$

This calculation involves only integer counting, gives a qualitatively useful first approximation to the $\mathbf{v}\cdot\mathbf{j}$ correlation, and can be corrected exactly with many fewer transformations than the one-step method described above. It can be seen that only negative $\mathbf{v}\cdot\mathbf{j}$ correlations can arise in this way, since the constraints on λ are always in the form of an upper bound on the absolute magnitude. The correction to match the exact phase space theory involves finding those $l\,j$ states allowed by angular momentum conservation but rejected by energy conservation at the centrifugal barrier, transforming only those to the helicity basis and removing their contribution from $p'(\lambda_1)$ to compute $p(\lambda_1)$. The states in question are analogous to those shown in Fig. 1 within the trapezoid defined by angular momentum conservation, but at higher l and j than the curved boundary. Particularly for low J, the number of such states excluded by the centrifugal barrier will generally be much smaller than the number not excluded.

III. Illustration by Simple Example

As an example of the equivalence of the state counting, consider a single dissociation channel of a parent molecule with total angular momentum J=2 into a pair of fragments with rotational angular momenta j_1=1 and j_2=1. The conventional state count proceeds by combining j_1 and j_2 to give resultant j, which in this case can take on values of 0, 1, or 2 according the triangle inequality $\Delta(j,j_1,j_2)$. For each j, there will be a range of orbital angular momenta l that satisfy the triangle inequality $\Delta(J,j,l)$. The nine possible $j\ l$ states are enumerated in the table at the right. Each of these $j\ l$ states has total J=2 and a corresponding additional $2J+1$-fold degeneracy.

***jl* states for *J*=2, j_1=j_2=1**		
j	l	count
0	2	1
1	1, 2, 3	3
2	0, 1, 2, 3, 4	5

$\lambda_1\lambda_2$ states for *J*=2, j_1=j_2=1		
λ_1	λ_2	count
-1	-1, 0, 1	3
0	-1 , 0, 1	3
1	-1, 0, 1	3

The same dissociation channel can be characterized by the helicity states of fragments 1 and 2, denoted by λ_1 and λ_2. The angular momentum constraints are now embodied in the inequalities $|\lambda_1| \le j_1$, $|\lambda_2| \le j_2$, and $|\lambda_1-\lambda_2| \le J$. In each case the inequality arises from a projection number bounded by the magnitude of the associated angular momentum. A enumeration of the $\lambda_1\ \lambda_2$ states consistent with the same J, j_1, and j_2 is shown at the left. Again, we have nine $\lambda_1\ \lambda_2$ states, each with total J=2 and five possible values of M. In this helicity representation, it is clear that all permitted values of λ_1 are equally likely in the phase space count, and the ratio 3:3:3 for λ_1=−1:0:1 corresponds to no $\mathbf{v}\cdot\mathbf{J}$ correlation, as can be verified by evaluating the sum in equation 7.

If the total angular momentum in this simple case is reduced to J=1, the seven allowed $j\ l$ states are shown in the table at the right. In this representation, it is hard to see that there is now a non-vanishing $\mathbf{v}\cdot\mathbf{j}_1$ correlation, although the count of $\lambda_1\ \lambda_2$ states in the table below shows that the two states missing, compared to the uncorrelated case above for $J = 2$, have total helicity $\lambda_1 - \lambda_2 = \pm 2$, which is not possible when the total J is 1. The relative probabilities of λ_1 are now 2:3:2 and the expectation value of $P_2(\mathbf{v}\cdot\mathbf{j}_1)$ is $-1/14$. These illustrations show the identity of state counts in the conventional $|j\ l\rangle$ basis and in the helicity $|\lambda_1\ \lambda_2\rangle$ basis when the upper bound on l comes from angular momentum conservation and not energy conservation at the centrifugal barrier.

jl* states for *J=1*, j_1=j_2=*1		
j	l	count
0	1	1
1	0, 1, 2	3
2	1, 2, 3	3

$\lambda_1\lambda_2$ states for J=1, j_1=j_2=1		
λ_1	λ_2	count
-1	-1, 0	2
0	-1 , 0, 1	3
1	0, 1	2

As a final example, suppose that for the kinetic energy of this product channel, the orbital angular momentum could not exceed 2, so that the single l=3 state needs to be removed from the phase space count. That is, $N' = 7$, but $N = 6$.This $|j\ l\rangle$ state $|2,3\rangle$ can be expanded as a sum of $|\lambda_1\ \lambda_2\rangle$ states according to Eq. 6. In this case, explicit evaluation of the Clebsch-Gordon coefficients shows that this $j\ l$ state has contributions from all seven helicity components with the following amplitudes, a_i:

$$|j\,l\rangle = \sum_i a_i\,|\lambda_1\lambda_2\rangle_i$$

$$|23\rangle = \frac{1}{\sqrt{10}}\left[|-1\,-1\rangle - |-1\,0\rangle - |0\,-1\rangle + 2\,|0\,0\rangle - |0\,1\rangle + |1\,-1\rangle - |1\,0\rangle\right]. \tag{9}$$

The probability of measuring $\lambda_1 = -1 : 0 : 1$ in the $j\ l$ state $|23\rangle$ is related to the corresponding squared amplitudes, which occur in the ratio of 1/5 : 3/5 : 1/5. The normalized $p'(\lambda_1)$ was 2/7 : 3/7 : 2/7 from the previous example including all seven l states. The corrected, but unnormalized helicity distribution for particle 1 is then $p(\lambda_1) =$ 2–1/5 : 3–3/5 : 2–1/5, which results in a weaker $\mathbf{v}\cdot\mathbf{j}$ correlation of $-1/20$ for the six states, compared to $-1/14$ when all l states are included. This is qualitatively expected, as the states with the largest l will generally impose a stronger constraint on the remaining angular momenta.

IV. Application to NCCN Photodissociation at 193 nm

Vector correlations have been measured in this laboratory for selected states of the CN photofragments from the 193 nm dissociation of NCCN.[9] Cline and Klippenstein have recently performed Monte Carlo evaluations of classical phase space integrals to estimate the statistical state-resolved $\mathbf{v}\cdot\mathbf{j}$ correlations relevant to this system.[4] The full results of the helicity-based phase space calculations will be presented later[10]. For now, the results of the approximate version of the present quantum phase space theory, which ignores centrifugal barriers, can be compared with Klippenstein's calculations in Table I at the end of this article. For these calculations, $p'(\lambda_1)$ was computed for selected states j_1, with $v_1 = 0$ and 1, averaged over coincident j_2, treating $v_2 = 0$ and 1 separately, for various NCCN total J. The helicity state counts were made assuming an available energy of 4700 cm^{-1} to compare to the calculations of Cline and Klippenstein. These state counting calculations took about 3 seconds on a Pentium PC. The $\mathbf{v}\cdot\mathbf{j}$ correlations, $\beta_0^0(22)$, calculated with this approximate method agree very well with the classical Monte Carlo method, particularly at low J, as one might expect. Both the trends and the magnitudes of the $\mathbf{v}\cdot\mathbf{j}$ correlations with total J and with the fragment j are reproduced correctly, except the small positive correlation calculated by Cline and Klippenstein at high total J and high fragment j, which is not reproduced in the present approximate calculations. This difference occurs for those channels where the centrifugal barrier should have the strongest effect. In general, the neglect of the centrifugal barrier does not appear to cause a serious problem in the estimation of vector correlations. The absolute state count and the rotational distributions will show more serious deviations due to the neglect of the centrifugal barrier. The corrected calculations, including the transformation into the helicity basis of the centrifugally forbidden states are deferred to a later article.[10] A comparison of the $v_1 = 1$ calculations are not shown here, but display similar agreement with the Cline and Klippenstein results.

Table I. Calculated vector correlations $\beta_0^0(22)$ for v = 0, j_{CN} selected CN fragments from NCCN: comparison of Monte Carlo classical phase space theory (CPST)[a] with helicity state count (HSC)

	$j_{CN} = 17$		$j_{CN} = 30$		$j_{CN} = 35$		$j_{CN} = 40$	
J_{NCCN}	HSC	CPST	HSC	CPST	HSC	CPST	HSC	CPST
coincident CN v = 0								
0	-0.056	-0.056	-0.154	-0.158	-0.243	-0.260	-0.363	-0.378
10	-0.045	-0.044	-0.140	-0.150	-0.223	-0.233	-0.329	-0.343
20	-0.028	-0.030	-0.115	-0.121	-0.169	-0.172	-0.242	-0.255
30	-0.021	-0.023	-0.076	-0.073	-0.109	-0.109	-0.151	-0.152
40	-0.016	-0.016	-0.043	-0.041	-0.057	-0.051	-0.076	-0.065
60	-0.001	0.000	-0.005	0.000	-0.007	0.005	-0.008	0.008
80	0.000	0.000	0.000	0.000	-0.000	0.004	0.000	0.018
coincident CN v=1								
0	-0.087	-0.091	-0.358	-0.386	-0.461	-0.486	—[b]	—
10	-0.071	-0.077	-0.300	-0.324	-0.418	-0.441	—	—
20	-0.044	-0.047	-0.180	-0.183	-0.289	-0.286	—	—
30	-0.026	-0.024	-0.076	-0.063	-0.119	-0.053	—	—
40	-0.009	-0.006	-0.022	-0.002	-0.024	0.062	—	—
60	0.000	0.002	0.000	0.017	-0.000	0.057	0.000	-0.080
80	0.000	0.002	0.000	0.013	-0.000	0.039	0.000	0.018
Thermal		-0.027		-0.084		-0.105		-0.145
Expt[9]	-0.08 ± 0.04		-0.15 ± 0.06		-0.21 ± 0.04		-0.23 ± 0.04	

[a] CPST calculations and thermal averages are the work of Cline and Klippenstein[4]; HSC is this work

[b] A dash indicates an energetically inaccessible state

The key result is that the observed vector correlation is about twice as large as the thermally averaged, statistical expectation, as noted by Cline and Klippenstein.[4] It seems very likely that this is a consequence of an additional constraint on the dissociation of the linear molecule, NCCN. In computing the state distribution, the total helicity of the two fragments is allowed to range between $+J$ and $-J$ of the parent molecule. In the axial recoil limit, where the radial velocity of the fragments far exceeds their tangential velocity, the combined helicity of the two fragments is closely identified with the projection of total J around the axis of the linear molecule, which necessarily vanishes. The spectroscopically populated levels of the predissociating NCCN $A\ ^1\Sigma_u^-$ and $B\ ^1\Delta_u^-$ states are reached by vibronically-induced transitions characterized by a single unit of vibrational angular momentum, K=1. If this body-fixed projection number is not mixed in the internal conversion to the ground state or in the separation of CN products, we should expect the total helicity to stay small, even in a thermal sample of NCCN with large values of total J. For this special case of linear molecule dissociation, the angular momentum conservation constraint in the helicity basis are even simpler than shown in Eq. 5 as the value of $\lambda_1 - \lambda_2$ is restricted to zero, rather than merely being bounded by $\pm J$:

$$N'_{linear}(E,J) = \sum_{v_1,j_1,\lambda_1,v_2,j_2,\lambda_2,m_J} \Theta[\ E - E_1(v_1,j_1,k_1) - E_2(v_2,j_2,k_2)] \times \Theta(0 - |\lambda_1 - \lambda_2|) \tag{10}$$

The vector correlations including this constraint are identical to those obtained for total $J = 0$, even in a room temperature sample. The $J = 0$ rows of Table I are in nearly quantitative agreement with the experimentally determined $\mathbf{v}\cdot\mathbf{j}$ correlation parameters, lending support to this notion of K restriction in a linear molecule leading to enhanced $\mathbf{v}\cdot\mathbf{j}$ correlation.

Further questions remain about the true available energy, the possible role of an exit barrier in the dissociation, kinetic shifts in the threshold for detecting CN fragments, and the relationship between the available energy, the state distributions, and the vector correlations. New experimental work and the extension of the theory sketched here are both in progress.[10] We are optimistic about resolving the speed-dependent $\mathbf{v}\cdot\mathbf{j}$ correlation in our next generation of Doppler spectroscopy experiments, which is related to the coincident j_2-dependent helicity distribution.

Acknowledgments

I thank Prof. Stephen Klippenstein for helping in the early stages of this work by convincing me that statistical theories had something to say about vector correlations. In the later stages he assisted with extensive discussion and a prepublication copy of reference 4. This work was performed at Brookhaven National Laboratory under Contract No. DE-AC02-76CH00016 with the U.S. Department of Energy and supported by its Division of Chemical Sciences.

References

1. P. Pechukas and J.C. Light, *J. Chem. Phys.* **42**, 3281 (1965); P. Pechukas, J.C. Light, and C. Rankin, *J. Chem. Phys.* **44**, 794 (1966); J.C. Light, *Disc. Faraday Soc.* **44**, 14 (1967).
2. J.C. Light, in *Atom-Molecule Collision Theory: A Guide for the Experimentalist,* R.B. Bernstein, ed., Plenum Press, New York (1979), and references cited therein.
3. I.-Chia Chen, W.H. Green, Jr., and C.B. Moore, *J. Chem. Phys.* **89**, 314 (1988), and references cited therein.
4. S. Klippenstein and J. Cline, *J. Chem. Phys.* submitted 1995.
5. R.N. Dixon, *J. Chem. Phys.* **85**, 1866 (1986).
6. M. Jacob and G.C. Wick, *Annals of Phys.* **7**, 404 (1959).
7. P.J. Dagdigian, H.W. Cruse, A. Shultz, and R.N. Zare, *J. Chem. Phys.* **61**, 4450 (1974).
8. C. Wittig, I. Nadler, H. Rewisler, M. Noble, HJ. Catanzarite, and G. Radhakrishnan, *J. Chem. Phys.* **83**, 5581 (1985).
9. M. Wu and G.E. Hall, *J. Photochem. Photobiol. A: Chem.* **80**, 45 (1994).
10. In preparation.